A Study on Mm-wave Multi-User Directional Beamforming Based on Measurements and Ray Tracing Simulations

F. Fuschini, M. Zoli, E.M. Vitucci, M. Barbiroli and V. Degli-Esposti

Abstract — **This study concerns the evaluation of beamforming techniques in multi-user indoor environment at the mm-wave frequency band of 70 GHz using both measurements and ray tracing simulations carried out in a furnished small-office environment. The goal of the work is twofold: (i) to evaluate ray tracing as a reliable directional channel model for beamforming assessment and for real-time assistance in the beam-searching phase, (ii) to evaluate simple beamforming schemes as means to enforce spatial division in a small-indoor environment. Results suggest that the considered ray tracing model can be reliable enough to reproduce the general performance trends of different beamforming schemes and to assist the beam-searching phase, therefore potentially reducing the related time delay and computational overhead.**

Index Terms— **Millimeter wave propagation, Multi User Beamforming, Ray Tracing, SDMA.**

I. Introduction

Electromagnetic propagation at mm-wave frequencies has different properties compared to propagation below-6 GHz, such as a much greater isotropic path-loss and a multipath structure that is often sparse and clustered [1]-[5]. Furthermore, due to the relatively low congestion of the spectrum in the 24-70 GHz range, mm-wave radio channels are likely to be dedicated to wideband, high-speed communications, which may have low signal-to-noise-ratio (SNR) compared to lower frequencies because of the wideband noise [1].

In presence of limited multipath richness and low SNR, multi-antenna communication schemes can hardly provide optimal spatial multiplexing gain, and therefore they should be used to implement beamforming (BF) solutions [3], [6], which can compensate for the heavy propagation losses by taking advantage of the directional properties of the channel.

In order to represent a valid enabling technology for the forthcoming 5G wireless systems, BF must be adaptive [7], i.e. beam-steering must be dynamically changed to track users' mobility and/or to cope with possible unexpected link blockage, that can be disruptive especially at millimeter frequencies [8], [9]. Furthermore, in a multi-user (MU) scenario, optimal beam-steering procedures should aim at boosting the received signal strength to each user while reducing the interference vs. the other users at the same time, to the extent that BF can potentially become a multiple access technique (Spatial Division Multiple Access – SDMA) complementing traditional solutions in the time (TDMA), frequency (FDMA) and code domain (CDMA) [10], [11].

To the authors' knowledge, time-variant and/or multi-user scenarios still represent open issues for adaptive BF strategies. In fact, state-of-the-art BF protocols are likely to be impractical when a large number of (mobile) users is taken into account: dirty paper coding [12] becomes computationally too heavy, zero-forcing (ZF) BF [4], [13], [14] can hardly rely on channel state information (CSI) because it might be imperfect or not up to date [15]-[17]. In light of these critical issues, simpler, sub-optimal, heuristic beamforming strategies are also being investigated [5], [18]-[21].

In this framework, this study deals with a class of BF algorithms (herein referred to as *directional BF*) that only take into account the directional properties of the channel to steer the main radiation beams of the antenna toward the proper directions [5], [19], [21]. Such methods are simpler, because they do not require full-CSI, i.e. the knowledge of the complex-valued MIMO channel matrix, and yet might approach full-CSI schemes in terms of performance in multipath-poor channels such as mm-wave channels [5]. Directional BF implementations however are often based on (exhaustive) search algorithms to select the best steering vector among a large codebook of pre-set vectors [17] [19], [22], which may lead to a heavy computational overhead, especially in presence of mobile users and when BF is applied at both link ends.

Therefore, further investigations are still necessary before international standardization bodies and research institutions can define robust and well-performing MU-BF algorithms [17]. From a propagation perspective, this entails the need for a deeper insight into the directional characteristics of the mm-wave channel, and especially into their impact on MU-BF performance.

Although ray tracing (RT) models are inherently suitable to account for the multipath nature of the channel, their actual reliability for the assessment/design of BF strategies in complex propagation scenarios cannot be automatically taken for granted. Since RT tools cannot accurately track the phase relations among the propagation paths, they are of little avail – if not in simple, ideal cases – when BF schemes requiring a full CSI must be considered. Conversely, RT can fairly reproduce the geometry and the attenuation for each path, and therefore it may represent in theory a helpful propagation

All the authors are with Department of Electrical, Electronic and Information Engineering, "G. Marconi" (DEI), University of Bologna, IT-40136 Bologna, Italy (e-mail: {franco.fuschini, marco.zoli5, enricomaria.vitucci, marina.barbiroli, v.degliesposti}@unibo.it)

engine for the prediction of signal-to-interference and noise (SINR) ratios in directional BF solutions. In practice, this possibility can also undergo some limitations that should be further investigated. It is generally agreed that because of the several impairments affecting RT simulators (e.g. imprecision in the environment and antenna description), their accuracy for path-loss modeling corresponds to a prediction error standard deviation of several dBs even in the best cases [23]-[27]. Moreover, SINR estimation requires path-loss assessment over multiple links, that could in the end results in a poorer prediction. This can be especially true when BF schemes must be simulated, since interference is often expected to come from the side lobes of the directive antenna patterns, which might suffer from inaccurate description in RT simulation.

Such problems are addressed in this manuscript through 3D directional channel measurements carried out in a small office environment in the 70 GHz band and RT simulations [28]. In particular, measured and simulated SINR distributions are computed and compared for a different number of active users (N_{AU}) and for three reference BF strategies, ranging from a basic solution where the antennas are simply oriented in the transmitter (Tx) - receiver (Rx) direction, to a cooperative policy where an exhaustive search for effective SINRs determines the antennas steering. Both BF at Tx side-only and joint bi-directional BF (i.e. applied to Tx and Rx) are considered.

Finally, RT assisted MU-BF is also outlined in this study as a way to use RT prediction not only to assess benefits and drawbacks of different directional BF strategies, but also to contribute to drive or assist the beam-searching phase therefore drastically reducing processing time.

Similar studies have been carried out and published in the recent past [4], [29], [30]. In [4] however, ZF-BF is addressed, whereas the attention is here turned to directional BF schemes. Furthermore, the BF analysis in [4] relies on channel measurements only, without any comparison with RT or other propagation models. In contrast, BF simulation in [29] is based on the RT-simulated channel only and only mono-directional BF solutions are considered. In [30] only single-user BF is addressed, and RT-assisted BF is assessed as a promising solution for future wireless systems, similarly to what concluded in this work for different BF schemes applied to a MU scenario.

For the sake of generality and simplicity, specific antenna-array topologies are not considered in the present work. The directive radiation pattern of the circular horn antenna used for the measurements is chosen as the reference pattern, and its main lobe is simply mechanically pointed toward different directions to simulate different beam-steering solutions, without changing the radiation pattern. Since the half-power beamwidth (HPBW) of the antenna is equal to 15°, it approximately corresponds to a broad-side array of few hundreds of isotropic elements, but of course the effect of side lobes and of polarization degradation – especially for very large steering-angles - of real arrays is not considered in the work.

The paper is organized as follows: the concept of the work is outlined in section II, whereas the experimental and the RT-based approach for the estimation of the channel's directional properties is presented in section III; the considered beamforming strategies and system simulation procedure are described in section IV. Results – including an assessment of the RT-assisted BF idea - are addressed in section V. Finally, conclusions are drawn in section VI.

II. Concept and Scope Of Work

Multiuser indoor beamforming is investigated in this study through a double-track, simulated/experimental approach following the general scheme sketched in Figure 1.

The directional properties of propagation at 70 GHz in a small-office environment have been first explored by means of both measurements carried out with a channel sounder (CS) and 3D RT prediction. Since the outcomes of the mm-wave radio channel characterization have been already presented in [28], they are just shortly referred to in the following section III.

The measured/simulated power angle profiles (PAP) provided by the directional channel estimation (i.e. the received power levels at the considered Rx locations for different orientation of the antennas) are then exploited to perform MU-BF system-level simulations based on multiple user-position "drops" in the considered office scenario where beam steering is enforced using three different strategies: Radial, Best-SNR and Best-SINR, as described in detail in section IV. The considered BF schemes are finally compared for different number of users in terms of overall SINR statistical distributions.

In the *measurement track* (on the left in Figure 1) the beam-steering decision algorithm makes use of the measured channel's PAP for the beam-searching phase and the SINR performance statistics are also derived from the measured channel.

In the *simulation track* (on the right in Figure 1) the beam-steering decision algorithm makes use of an RT-simulated channel's PAP, and the SINR statistics are also derived from the RT-simulated channel.

Comparison between the measurement- and the simulation-track performance suggests that RT can represent a fair propagation model for BF system simulation (BF simulation validation). This is different from assessing RT as a mere propagation prediction tool (propagation validation).

Furthermore, a mixed solution is also considered (box at the bottom, center of Figure 1), where beam steering is driven - at least partly - by the RT prediction but the SINRs performance statistics are computed using the measured PAPs. This case corresponds to studying a so-called RT-assisted BF technique, where the system partly or totally skips the beam-searching phase complexity and processing time, with corresponding feed-back loop Rx-to-Tx, and relies on embedded RT-prediction to find the optimum beam steering solution for each users location configuration. This hybrid solution is discussed in detail in section V.C.

III. Directional Channel Estimation

A. Channel Sounder Measurements

The measurement scenario is a 21 m^2 small office where 6 Rx and 2 Tx positions (Tx1 and Tx2 in Figure 2) are considered. All Tx-Rx links are in line-of-sight (LoS) with no people present [28].

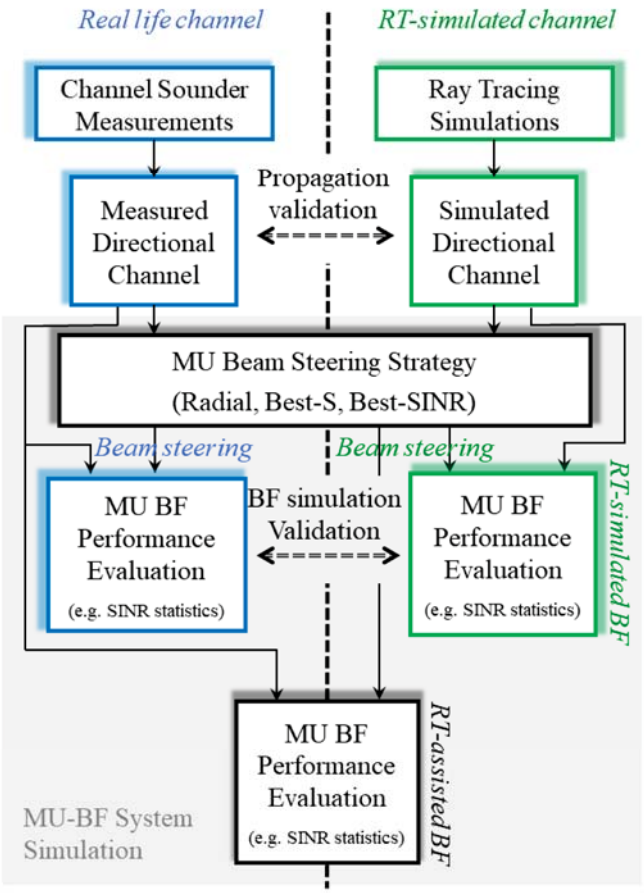

Figure 1. Logical block scheme describing the adopted methodology for the analysis and assessment of MU-BF capabilities.

The measurements have been performed with a custom mm-Wave CS developed at TU Ilmenau [31] based on an UWB M-sequence chip-set, offering a 3 dB instantaneous bandwidth of 4 GHz after calibration. Results presented in this paper refer to a transmitter power equal to 0 dBm. The Tx/Rx antennas are cylindrical horn antennas with HPBW=15° and a maximum gain of 20 dBi, and have been mounted on rotating positioners at both link ends. Although the antennas are dual polarized, the MU-BF analysis is here limited to the vertical polarization case. In order to emulate a smart indoor access point, the Tx can mechanically scan both elevation and azimuth, whereas the Rx scans in azimuth only (Figure 2). When the Tx is located in the a corner of the room (Tx1 location), it sweeps along [-75°, 75°] of elevation and [-15°, 75°] of azimuth (namely angle of departures, AOD). The Tx2 position corresponds to the Tx located over the table in the middle of the office [28], sweeping over [-75°,75°] in both azimuth and elevation. The Rx sweeps along the full [0,360°] range of azimuth (namely angle of arrival, AOA). The spatial scanning resolution is equal to 15°.

Finally, measured data are stored as complex channel impulse responses (CIR) and collected for every pair of Tx/Rx pointing directions. The 6 different Rx positions have been measured one by one sequentially using a wheeled mobile cabinet supporting the CS Rx unit and all the data have then been gathered to create the multi user data set.

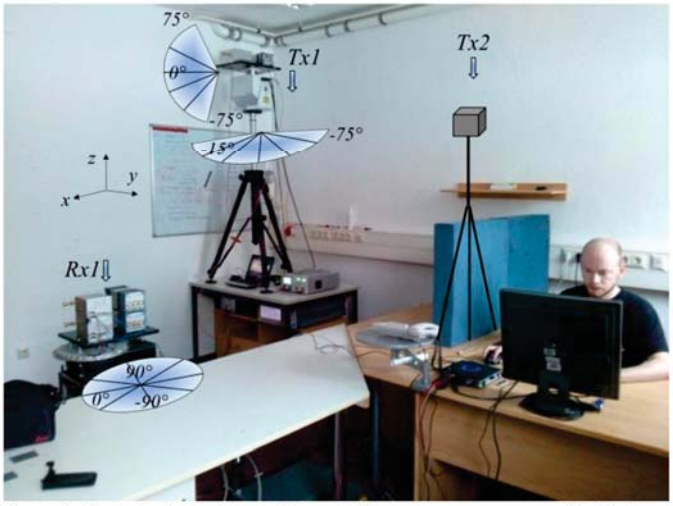

Figure 2. Picture of the room with overlaid measurement set-up for Tx1 and Rx1 (the position of Tx2 is also sketched).

The collected measurement data are then exploited to drive different BF schemes (as described in section IV.A) based on the power levels conveyed at the Rx locations for the different antenna pointing directions (11×11 AOD for Tx2, 11×5 AOD for Tx1, and 24 AOAs for any Rx). The received power values are computed by adding up the intensities of the signal contributions in the CIRs standing out against the noise level (equal to -150dBm).

In this work, we focus mostly on results with a synthetized omnidirectional Rx, i.e. the power received over the 24 Rx angular slots is summed up to form an omnidirectional azimuthal diagram. BF is performed only at Tx side, and it is named "mono-directional BF" (or "mono-BF") in the following. This may be reasonable considering the capabilities of today's access points, with respect to mobile or tablet devices. In case the Rx antenna directivity is also taken into account, the beam search procedure must be performed over both the AOD and the AOA, at the same time. This case is referred to as "bidirectional-BF" (or "bi-BF") in the following.

Because of the spatial selectivity at both link ends, bi-BF is likely to outweigh mono-BF in terms of effectiveness, but it also entails a heavier impact on users' terminal cost and design complexity. In any case, the analysis carried out in the following section is limited to a performance assessment, and any issue specifically related to practical implementation is not being addressed at the moment.

B. Ray Tracing Simulations

In addition to the measurements, RT simulations have been carried out in the same environment using a custom 3D RT

tool, specifically conceived for indoor environments and able to take into account all the important electromagnetic propagation mechanisms such as specular reflection, diffraction, transmission and diffuse scattering. In particular, diffuse scattering is implemented adopting the effective roughness model [32], previously tuned and parametrized for mm-Wave frequency bands [28]. The RT geometrical database consists of a 3D representation of the small office including the building frame and openings, the hydraulic and electric installations and the largest furnishings objects (e.g. desks, chairs, cupboards and cabinets). Further details can be found in [28]. Moreover, isotropic and omnidirectional radiation patterns have been first considered for the Tx and the Rx antennas, in order to catch all the rays by means of a single RT run. Then, the directional CIRs and PAPs have been computed weighting the intensity of the rays with the 3D directional radiation patterns for the different antenna orientations. Due to the limited information available about the antenna radiation characteristics (radiation patterns available only on 2 planes), interpolation of the E- and H-plane antenna diagrams [33], [34] has been applied to extract the required 3D patterns.

IV. Beamforming System Simulations

System-level simulations take into account exhaustively all the possible configurations of the N_{AU} active users (AU) in the small-office environment, i.e. a sequence of different "snapshots" (or "drops") is considered.

Each drop considers a different arrangement of the N_{AU} Rxs over n possible locations (up to a maximum of n=6, which are the Rx locations selected from the measurements described in [28]). The overall number of combinations amounts to:

$$N_D = \binom{n}{N_{AU}} = \frac{n!}{(N_{AU})!(n-N_{AU})!} \quad (1)$$

After that, the best set of beam orientations (i.e. the best beamforming solution) is then identified for each drop according to different criteria as described in the following sub-section.

A. SDMA BF schemes

For each Rx location drop, a beam search is performed all over the angular discrete set to achieve the *best BF solution*, i.e. the best set of N_{AU} beams, according to 3 different techniques:

✓ Radial BF method: a non-cooperative solution where the antennas radiation lobes are simply steered in the Tx-Rx direction for each active link. This scheme is clearly very simple but requires an indoor localization technology. Beam search is actually not necessary in this case, since the antennas' steering just depends on their positions, without the need for any spatial scanning;

✓ Best-SNR BF method: beam search is based on the received power level (S), regardless of interference. Practically, a feasible solution can exploit an uplink channel state information (CSI) feedback to inform the Tx about the received power from all AUs. An "oracle-based" solution is considered for the sake of simplicity for all the MU-BF simulations, meaning that the CSI is assumed known on the basis of measurements and/or RT simulations.

✓ Best-SINR BF method: is an interference-aware, cooperative beam-search solution based on the ratio between received power and interference levels (I). In this case, the price to pay is a more challenging CSI estimation, which may lead to large overhead or time consuming signaling. An "oracle-based" solution is again considered for the sake of simplicity.

B. Beam search optimization

In a MU scenario, a high aggregate throughput represents a major goal for an effective BF technique. At the same time, unbalanced SINR distributions should be also avoided, in view of a "fairness principle" that should be granted to the active users. For example, a BF solution generating similar SINR levels should be preferred to another with the same average SINR but different (unbalanced) SINR values for the different users.

Therefore, the best BF solution should be selected so that the SINRs experienced by each user is as high as possible, while at the same time all the users have similar SINRs. Hence, the average SINR for all users should be at a maximum, whereas the variance should be at a minimum. It is possible that a single user could achieve a higher SINR with another BF solution, but this would occur to the disadvantage of other users who would get a lower SINR.

In order to accomplish this target, a metric ρ_ψ is defined as the difference of the mean with the standard deviation as follows:

$$\rho_\psi = \langle \mathrm{SINR} \rangle_\psi - (\sigma_{\mathrm{SINR}})_\psi \quad (2)$$

where <·> and σ stand for mean value and standard deviation respectively, and $\psi=(\psi_1, \psi_2,\ldots, \psi_{NAU})$ represents a set of N_{AU} spatial directions describing the beam steering arranged at the Tx towards the different AUs. Despite the discussion is here limited to the mono-BF case for the sake of simplicity, ρ_ψ is still meaningful in the bi-BF case provided that ψ also includes the further N_{AU} beam pointing directions of the directional antennas at the AUs.

The beam search optimization method proposed here aims at finding the best beamforming solution for each snapshot – i.e. the set of beam steering directions $\bar{\psi} = (\bar{\psi}_1, \bar{\psi}_2, .., \bar{\psi}_{N_{AU}})$ maximizing the metric ρ_ψ. For each snapshot, the best BF solution $\bar{\psi}$ is selected among the collection Ψ of all the possible N_{AU}-ples of beam steering angles: for example, considering the Tx2 location with mono-BF, the searching domain Ψ consists of $(11\times11)^{N_{AU}}$ possible cases, and the best solution $\bar{\psi}$ is selected among them so as to maximize the value of ρ_ψ. This procedure is repeated for each drop, i.e. $N_D \times N_{AU}$ SINR values are eventually collected and represent the statistical base for the analysis carried out in section V.

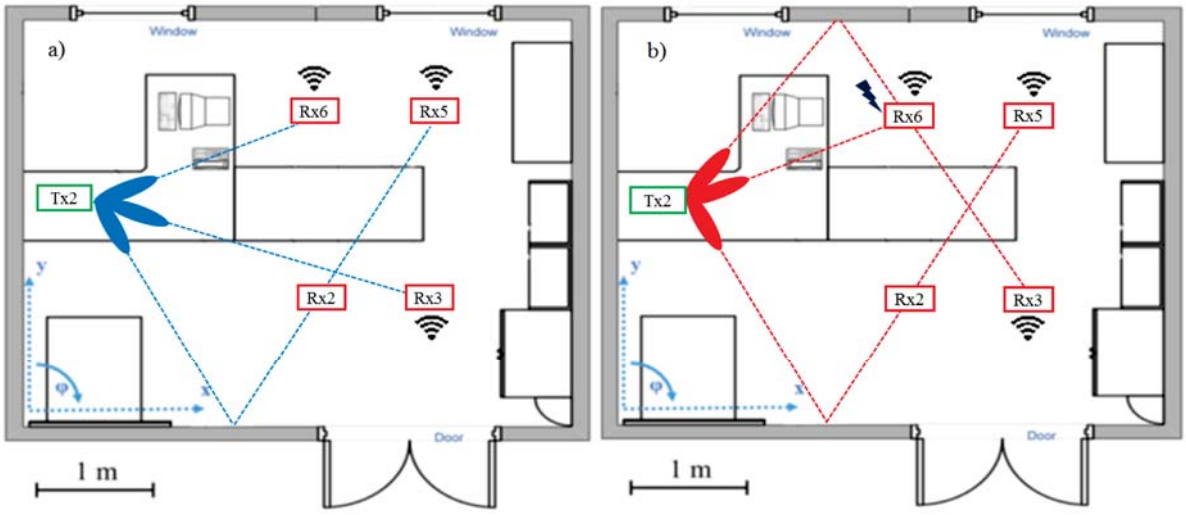

Figure 3. Rx6, Rx5 and Rx3 (N_{AU}=3) served by TX2 according to Best-SINR (a) and Best-SNR (b) with mono-BF RX.

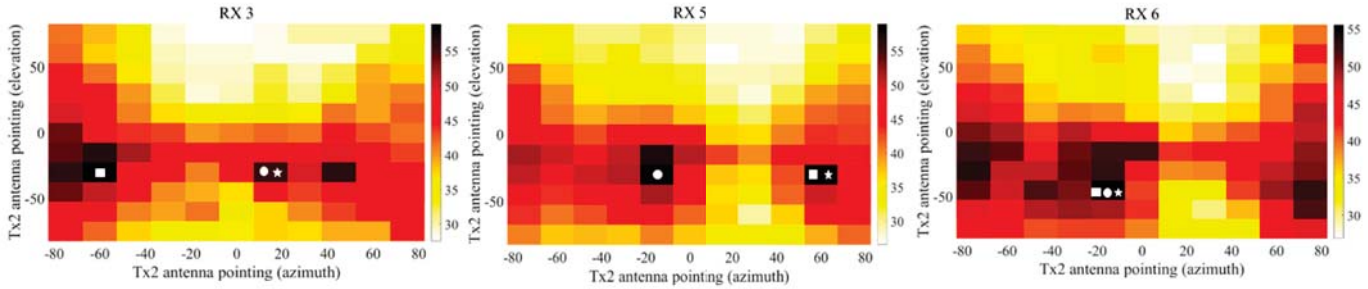

Figure 4. SNR angular distributions for the directive wireless links between Tx2 and Rx3, Rx5 and Rx6. Pointing directions of the beam for the different BF schemes are represented with a circle (Radial), square (Best-SNR) or star (Best-SINR).

The same optimization procedure holds for the Best-SNR method, simply substituting the SINR average value with $\langle S \rangle_\psi$ in eq. (2). It is worth mentioning that transferring the fairness constraint into the Best-SNR scheme by simply substituting $(\sigma_{SINR})_\psi$ with $(\sigma_S)_\psi$ would be questionable. In fact, the balance among the received power levels would not automatically entail any fairness in the quality of services, which is somehow related to the SINRs rather than to the SNRs only. Therefore, the Best-SNR scheme has not been conditioned by any fairness requirement, and the cost function just consist of the maximization of the average SNR.

Due to memory limitations, a maximum of 4 AUs have been considered for the mono-BF case, and 3 AUs for the bi-BF case. For the same reason, the analysis is restricted to single-beam schemes, i.e. each AU can just rely on one (two) properly steered beam(s) in the mono- (Bi-) BF case. Although a multi-beam approach may result in improved system performance [29], especially in terms of robustness to unpredictable link blockage that can occur in dynamic scenarios, it would result in a disruptive increase in the computational burden when added to the multi-user feature.

C. Case study

In order to clarify the behavior of the different beam-search schemes, a preliminary investigation has been carried out over the spatial domain in the mono-BF case and for N_{AU}=3 (Rx3, Rx5 and Rx6 in Figure 3). The Tx2 location is considered, which benefits from a greater degree of freedom in beam steering as the Rxs locations are spread over a wider spatial angle compared to Tx1. The pointing directions selected at the end of the different BF strategies are marked in Figure 4 with a circle (Radial), a square (Best-SNR) or a star (Best-SINR). Finally, TABLE I summarizes the outcomes of the BF schemes in terms of SNR, SINR and AOD for the three receivers. The large differences between the SINR and SNR values in TABLE I highlights that interference represents a heavy limitation, greatly affecting the BF strategies as briefly discussed herein.

In spite of its simplicity, the RAD scheme yields the highest SINR (Rx3, TABLE I); nonetheless, it also provides the lowest value (Rx6, TABLE I), since it does not take fairness into any consideration. Of course, the closer the AUs (like Rx5 and Rx6 in Figure 3), the worse the performance of the RAD solution.

The Best-SNR scheme always conveys the largest SNR (Figure 4, TABLE I), but it still spreads the SINR values over a quite large range, since interference is again neglected by the beam search procedure. This is clear in Figure 5, where the power delivered to Rx3 and the corresponding interference simultaneously inflicted on Rx6 are plotted against the

possible azimuthal pointing of the Tx2 antenna (elevation is set to -30° for the sake of simplicity). Maximizing the signal intensity to Rx3 (Best-SNR) does not represent the best choice if interference mitigation must be also pursued. In contrast, the Best-SINR strategy ensures the best outcomes overall, since it trades off – by definition – the aggregate SINR against the fairness target (Figure 5).

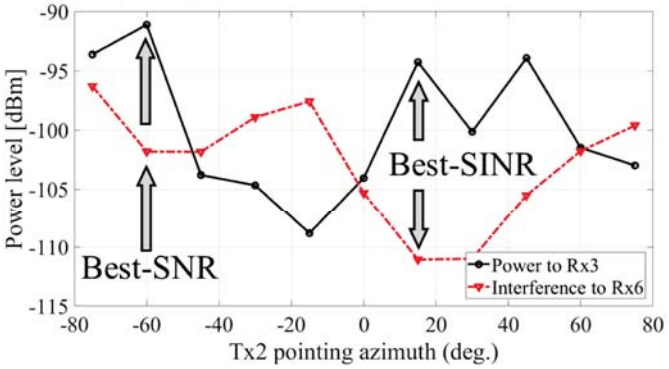

Figure 5. Signal intensities at Rx3 and corresponding amount of interference to Rx6 as the Tx2 antenna sweeps over the azimuth range (elevation is fixed to -30°)

As shown in Figure 3a), the Best-SINR scheme still schedules Rx6 and Rx3 along the direct paths, which can convey a fair amount of power keeping the mutual interference under control since they benefit from a sufficient spatial separation. Conversely, a different strategy is enforced for Rx5, which is supplied through a single reflection on the lower wall (Figure 3a), thus avoiding the heavy impairment on Rx6 that occurs in the RAD case, as already pointed out. In the end, the three link are arranged on quite powerful paths with limited spatial overlapping, corresponding to a satisfactory balance between the SINR values, equal to about 7 dB for each user (TABLE I).

Finally, comparing the SNR values in TABLE I shows that the strongest signal contribution arriving at Rx3 and Rx5 corresponds to a single bounce on the lateral walls (Figure 3a) rather than to the direct path. This can be explained by the limited rotation freedom of the receiving antennas, which can scan the horizontal plane only. Since the antennas are placed at different heights, the main radiation lobe at the Rx side can therefore never point towards the Tx, and the angle of arrival of the direct path never benefit from the total effective aperture of the receiving antenna. Conversely, a reflected path can experience a more favourable AoA, which may compensate for the longer travelled path and the reflection loss in some cases.

TABLE I
CASE STUDY: SUMMARY OF THE DIFFERENT BF METHODS

		Rx3	Rx5	Rx6
SINR (dB)	Best-SINR	6.8	7.2	6.8
	Best-SNR	9.9	6.1	4.3
	RAD	12.5	6.8	2.9
SNR (dB)	Best-SINR	55.7	59	55.5
	Best-SNR	58.9	59	55.5
	RAD	55.7	58.4	55.5
AOD (az.°,el.°)	Best-SINR	(15, -30)	(60, -30)	(-15, -45)
	Best-SNR	(-60, -30)	(60, -30)	(-15, -45)
	RAD	(15, -30)	(-15, -30)	(-15, -45)

From this example, it is evident that the problem of enforcing SDMA is not a simple one: different paths offer multiple degrees of freedom, but at the same time, also a source of interference and both effects must be taken into account.

V. RESULTS

A. BF performance based on channel measurements

Figure 6 shows the cumulative distribution functions (CDFs) of the SINR over all simulation drops and users when the considered BF schemes are applied at Tx2 in presence of 2 and 3 AUs.

Regardless of the BF algorithm, the increase in N_{AU} corresponds to a worse SINR distribution, i.e. the CDFs undergo a left-shift of few dBs. This is actually not surprising, since steering the beams in "safe directions" becomes harder and harder as the users' number rises up. In fact, a larger users' density entails a closer proximity among them (at least on the average), and therefore setting the beam in order to convey power to the target user only becomes step by step less effective.

The RAD and Best-SINR schemes achieve similar average performance in the considered scenario, but the RAD CDFs can reach a SINR of 18dB and 24dB outperforming Best-SINR in a limited set of cases, due to the absence of any requirement on SINR balance.

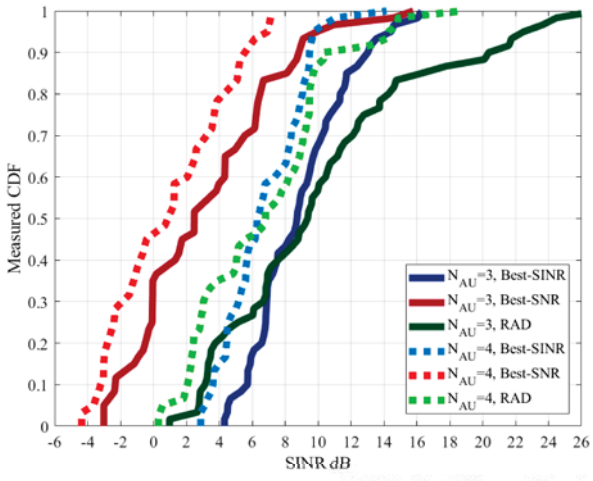

Figure 6. Comparison of SINR experimental CDFs for different BF schemes (Tx2, mono-BF). Solid curves are for 3 AUs and dashed lines for 4 AUs.

Because of the constraint on fairness applied to the Best-SINR beamforming method, the corresponding CDFs in Figure 6 rise at a steeper rate compared to the RAD and Best-SNR strategies. The users' SINRs gathered over the drops combination are spread over a narrower range when the beam-

steering is driven by the Best-SINR strategy, that exactly means a greater fairness is achieved.

The same effect can be highlighted by first computing the standard deviation (σ_{SINR}) of the N_{AU} SINR values returned by the beam search algorithm for each drop, and then drawing the CDF from the final set of N_D σ_{SINR} samples. This is represented in Figure 7, where the fairness of the Best-SINR solution results in a CDF much closer to the vertical axis.

In Figure 8, a comparison of mono-BF and bi-BF SINR CDFs is shown for Tx2 with N_{AU}=2 (a) and N_{AU}=3 (b). Thanks to the combined space-selectivity at both Tx and Rx, bi-BF attains a SINR gain over mono-BF, equal to about 15 when the Best-SINR strategy is applied to the small office environment under test. Basically, by performing BF at both link-ends, Best-SINR can benefit from a huge number of degrees of freedom - beam-steering solutions - to achieve low-interference links.

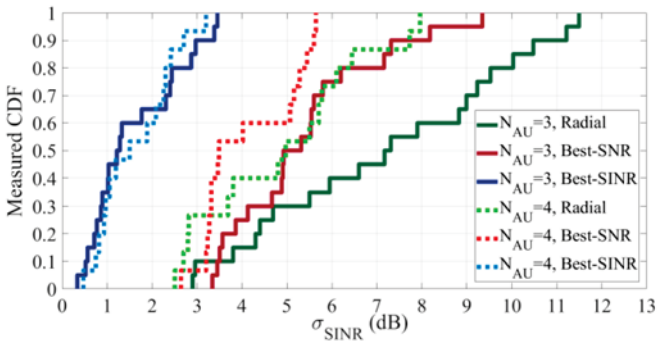

Figure 7. Comparison of σ_{SINR} experimental CDFs for different BF schemes (Tx2, mono-BF). Solid curves are for 3 AU and dashed lines for 4 AU.

In contrast, worse users configuration benefit from a much lower SINR improvement if the RAD method is applied. In fact, radial pointing basically provides low SINR when the users are spatially close each other's, and the corresponding impairment on SINR values is only slightly reduced if beamforming is performed at both link ends, although this also depends on the antenna radiation beamwidth.

All results based on the amount of experimental data collected in the small office are summarized in TABLE II including SINR statistics (mean and standard deviation) over different Tx positions for different BF methods. Best-SINR and RAD show the highest mean SINR, whereas Best-SNR has worse performance. Moving from N_{AU}=2 to N_{AU}=4 with mono-BF, the mean SINR decreases by nearly 7 dB due to the higher average interference.

Tx2 results are generally better because Tx1 is located in the corner of the room with half the field of view over the environment than Tx2 and therefore less headroom for BF to achieve a good space division. As already discussed, Best-SINR achieves a lower SINR standard deviation overall, because it is specifically conceived to pursue fairness too.

Investigations carried out in [35] and [36] achieved average SINR values equal to about 15 dB in the mono-BF case and for N_{AU}=2. Owing to the several differences in terms of frequency (60GHz [35] and 2.4GHz [36]), propagation conditions (a large room is experimentally addressed in [35], whereas the 802.11ad model for conference room is simply assumed in [36]), antenna layout (arrays in [35], [36]) and beamforming scheme (based on full CSI in [35], [36]), such results are in fairly good agreement with the corresponding ones in TABLE II.

Finally, including the realistic SINR data into Shannon channel-capacity formula we achieve on average 3 bps/Hz, 4 bps/Hz and 6 bps/Hz for N_{AU}=4, 3 and 2, respectively by only using Best-SINR mono-BF SDMA without other division or coding schemes.

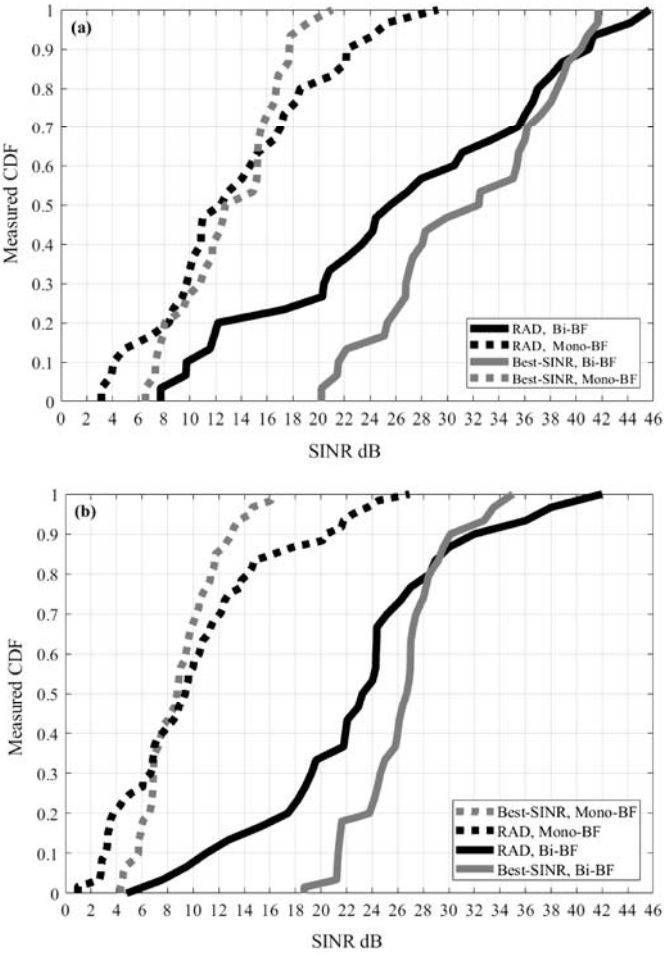

Figure 8. Comparison between mono- and bi-BF SINR experimental CDFs for N_{AU}=2 (a) and N_{AU}=3 (b).

TABLE II
GLOBAL SINR STATISTICS FOR DIFFERENT BF SCHEMES.

N_{AU}	BF Scheme	Avg. SINR (dB)		Std. Dev. of SINR (dB)	
		Tx1	Tx2	Tx1	Tx2
2	Best-SINR mono-BF	11	13	4	3
	Best-SINR bi-BF	31	33	7	8
	Best-SNR mono-BF	5	8	6	5
	BEST-SNR bi-BF	16	17	11	10
	RAD mono-BF	10	14	6	7
	RAD bi-BF	24	27	12	13
3	Best-SINR mono-BF	6	9	2	3
	Best-SINR bi-BF	20	26	6	4
	Best-SNR mono-BF	4	3	4	4

	BEST-SNR bi-BF	12	15	10	8
	RAD mono-BF	5	10	6	7
	RAD bi-BF	18	22	12	9
4	Best-SINR mono-BF	3	8	2	2
	Best-SNR mono-BF	1	2	4	3
	RAD mono-BF	4	7	6	4

B. BF performance based on channel Ray Tracing simulation

Beamforming simulations have been consistently repeated based on the RT-simulated double-directional channel. Results are shown in Figure 9 where the RT-based SINR CDFs (dotted lines) are shown to match quite well the measurement-based SINR CDFs (solid lines) for 2, 3 and 4 AU.

As shown in TABLE III, the root-mean-square-error (RMSE) of the RT-based BF simulations SINR with respect to measurement-based BF simulations is of about 3dB. By increasing the number of AUs the RMSE raises slightly by 1-2dB. Regardless of the considered BF scheme, the RMSE is always kept below 5 dB and this suggests that RT provides a rather satisfactory multidimensional characterization of the radio channel in the investigated scenario [28], and also a reliable tool for the statistical evaluation of beamforming schemes exploiting the directional properties of the radio channel.

However, by computing AOD pointing errors between measurement-based and RT-based BF directions for the reference Best-SINR, mono-BF technique, a mean error of about 20° and a maximum standard deviation of 30° in Azimuth and 50° in Elevation have been found. Besides the considerations examined in [28], two further reasons may explain this mismatch issue.

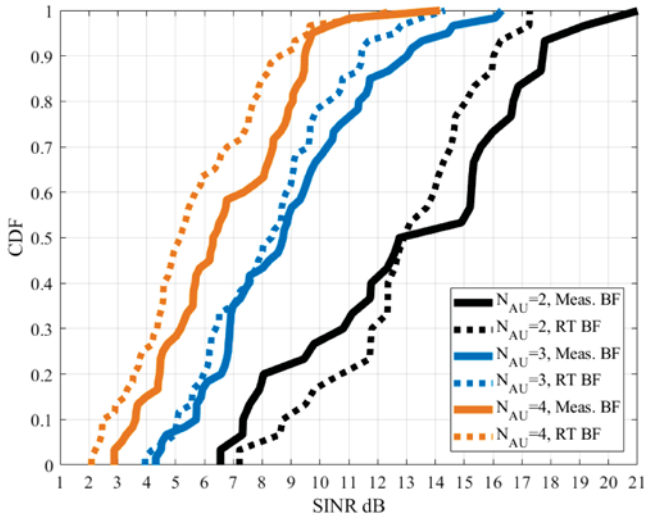

Figure 9. SINR CDFs comparison between measurements and simulations with N_{AU}= 2, 3 and 4 for Tx2, mono-BF according to Best-SINR BF scheme.

The first relates to the inherently challenging nature of the considered small office scenario. As previously pointed out, the direct path not always carries the greatest power, and some different rays with similar intensity are always present. This may seriously affect RT-based BF, because errors of few dBs in the prediction of the rays intensities (which are quite common) can (mis)lead the selection of alleged optimal steering directions which can turn out to be far from being really optimal when compared to the measurement-based BF results. Furthermore, the possible positions of the Tx (on a lateral wall or in the upper corner) do not represent the best choice for the spatial division of the users, which are always seen by the Tx under a narrower solid angle with respect to the case where the Tx is in a more central ceiling position. The limited angle diversity also contributes to the beamforming errors, which then result in the signal-to-interference prediction inaccuracies. In some way, such an environment may represent a sort of lower bound for RT-based beamforming.

TABLE III
BEAMFORMING BASED ON RT-SIMULATED CHANNEL VS. BEAMFORMING BASED ON MEASURED CHANNEL: OVERALL SINR ERROR

N_{AU}	BF Scheme	SINR RMSE (dB)	
		Tx1	Tx2
2	Best-SINR mono-BF	2	3
	Best-SINR bi-BF	3	2
	Best-SNR mono-BF	2	3
	Best-SNR bi-BF	3	3
	RAD mono-BF	2	2
	RAD bi-BF	4	2
3	Best-SINR mono-BF	2	2
	Best-SINR bi-BF	4	3
	Best-SNR mono-BF	3	4
	Best-SNR bi-BF	5	5
	RAD mono-BF	3	4
	RAD bi-BF	4	4
4	Best-SINR mono-BF	3	3
	Best-SNR mono-BF	5	4
	RAD mono-BF	3	4

The second reason is that RT shows better performance when required to estimate the useful power (i.e. conveyed at each AU through the dedicated beam) compared to its accuracy in the prediction of the interference level (i.e. the power at each AU coming from the beams designed for the others). This was checked by computing RT prediction errors at optimum beam pointing for received power and interference at each AU separately, resulting in mean error (error standard deviation) of 2 dB (2 dB) for the former, and 6 dB (10 dB) for the latter. Probably, the interference is much more dependent on minor, multiple-bounce paths and secondary antenna pattern lobes that are not accurately described in RT simulation. In particular, the RT antenna is described using 3D pattern reconstruction [33], [34] from 2D radiation diagrams, and therefore secondary, off-axis lobes are subject to interpolation errors. The larger interference consequently affect the SINR prediction, thus often preventing RT from identifying the really optimal beam steering directions.

C. RT-driven and RT-assisted BF

The concept of RT-driven/assisted BF was first coined in [29], and refers to the use of RT for real-time radio channel prediction to replace or assist the beam searching phase. Although the idea will require more extensive and application-oriented studies, this section provides at least a proof-of-concept, where the concept is described in some detail and assessed using measurements instead of simulations only as done in [29].

Localization techniques capable of achieving errors below 1m are likely to become available in forthcoming 5G networks thanks to the large bandwidths, high carrier frequencies and the simultaneous presence of multiple links at different frequency bands [37]-[39]. Moreover, accurate environment databases will be more and more readily available, through either download from the internet [40] or smart mapping techniques (e.g. based on laser scanning [41]). Thanks to the assets mentioned above, real-time RT prediction of the directional properties of the channel for multiple users could become feasible to ease beam-searching in directional BF techniques. Due to the limited directivity of the antennas, even in pencil-beamforming solutions based on very large arrays, and to the critical SINR requirements, the system will not be able to selectively use minor paths, but only dominant paths (or clusters) corresponding to LoS or single-bounce rays. Therefore, RT-assisted BF should not require very accurate, multiple-bounce RT simulation, nor a very detailed representation of the environment.

Real-time RT prediction on today's computing platforms in limited indoor environments can be performed very fast. It could even be carried out off-line by dividing the environment into pixels, pre-computing double directional channel information for every pixels' pair representing possible terminals locations and storing the result into a look-up table.

Channel variations due to terminal mobility can be also "predicted" by RT, because localization techniques can estimate the speed and therefore the future location of the user to some extent, while measurement can only sound the current state of the channel. In case of abrupt changes due to human blockage for instance, since RT-predicted information on the 4-5 strongest paths can be easily computed in one shot and stored, RT could still help in finding the second-best steering vector in a short time and therefore promptly restoring the link quality.

The RT-driven/assisted BF concept is evaluated for the Best-SINR mono-BF case, performing the following steps for each Rx location drop.

a) the Best-SINR BF method is run based on the measured channel in order to identify within the set of all possible BF solutions Ψ, the optimum solution:

$$\bar{\psi} = \left(\bar{\psi}_1, \bar{\psi}_2, ..., \bar{\psi}_{N_{AU}} \right) \tag{3}$$

i.e. the set of N_{AU} beams that achieve the best global performance metric ρ_Ψ from equation (2) based on the measured channel.

b) the parameter ρ_ψ is re-computed based on the RT-predicted channel for all possible beam-steering solutions (i.e. sets of N_{AU} beams chosen over the discrete angular set), and the ρ_ψ values are then sorted in descending order. The first solution in the list is therefore the Best-SINR BF solution based on RT:

$$\bar{\phi} = \left(\bar{\phi}_1 ..... \bar{\phi}_{N_{AU}} \right) \tag{4}$$

such solution achieves the best ρ based on the simulated channel, $\rho_{\bar{\phi}}$. Two different techniques are then evaluated, as explained here below.

1) RT-driven BF

Beamforming is assumed here to rely completely on RT and therefore BF solution (4) is chosen for each Rx locations drop. To evaluate this technique, for each drop we compute ρ for solution (4) using the measured channel instead of the RT-simulated channel, $\rho_{\bar{\phi}}^{(M)}$, where the subscript and the superscript indicate that the BF solution is found using RT but the performance metric is evaluated using the measured channel, respectively. Then we compute the error:

$$E_\rho = \rho_{\bar{\phi}}^{(M)} - \rho_{\bar{\psi}} \tag{5}$$

Such error indicates how much worse the RT-driven BF solution is with respect to the optimal BF solutions derived from the real channel. By collecting errors for all Rx positions drops we are able to derive the error statistics reported in TABLE IV, left-hand side. Unfortunately, results are not very good, with a 50th percentile error of about 6 dB and a 90th percentile equal or greater than 9 dB in terms of ρ. This is in line with the significant pointing errors found in section V.B. Therefore by using RT to directly pilot beam-steering we can expect to suffer an average SINR degradation of about 6 dB vs. an exhaustive search based on the real channel, at least in a challenging small-indoor environment such as the one considered here.

2) RT-assisted BF

This technique is based on two further stages. In the first stage RT is used to restrict the beam-searching angular set to a limited domain; in the second stage the actual beam-searching is performed over the restricted angular domain on the base of the measured channel. If the restricted angular range contains solution (3) then there is no performance degradation vs. an exhaustive search, but beam-searching time is drastically reduced.

During the first stage, for each Rx drop a BF solution subset is extracted from the RT-derived list described at point b) above by selecting all solutions with a ρ_ψ within a 3dB degradation with respect to $\rho_{\bar{\phi}}$. Then, Best-SINR beam-

searching is run over this restricted set of solutions based on the measured channel to single out the best one. Error statistics are derived in the same way as for technique 1).

Results shown in TABLE IV, last two columns, show that by doing so the error (5) is more than halved, with a mean error of about 3-4 dB with respect to the exhaustive search.

Moreover, considering that the restricted list found during the first stage always includes less than 100 BF solutions, the overall search domain for the second stage is reduced by a factor of at least 150 and 17700 for N_{AU}=2 and N_{AU}=3, respectively, with a proportional dramatic reduction of beam-searching time.

All considered it can be concluded that, while double-direction RT prediction is not accurate enough to really pilot beam-steering in a small indoor environment, it can still be an effective tool to help the BF algorithm to find an effective solution in a short time. However, further studies are required to fully assess the validity of this concept in practical system setups and in a wider range of propagation environments.

TABLE IV
RT-DRIVEN/ASSISTED BF ERROR STATISTICS.

N_{AU}	Tx	RT-driven BF		RT-assisted BF	
		50th percentile Eρ	90th percentile Eρ	50th percentile Eρ	90th percentile Eρ
2	Tx1	6 dB	14 dB	4 dB	6 dB
	Tx2	4 dB	9 dB	3 dB	5 dB
3	Tx1	6 dB	14 dB	3 dB	6 dB
	Tx2	6 dB	14 dB	4 dB	6 dB

VI. CONCLUSIONS

In this work, multi-user beamforming is investigated in a small indoor mm-wave environment. In particular, the performance of simple beamforming schemes is assessed taking into account the wireless channel directional characteristics, which are derived from both measurement and ray tracing simulations. Ray tracing seems to be a fairly effective tool for the statistical evaluation of the general performance of the different beamforming solutions.

Measurement and simulation analysis shows that the signal to interference ratios reduce for increasing number of users, to an extent that space division multiple access alone might be ineffective for reliable, high-speed communications. Improvements can be of course achieved if very narrow beams are adopted and/or in case beamforming is carried out at both link ends, which has turned out to raise the signal to interference levels up to 15-20 dB in the considered cases. Further investigations are needed to confirm these conclusions for different scenarios such as larger and/or more crowded environments.

Among the considered beamforming schemes, the Best-SINR solution, that mimics an exhaustive-search algorithm selecting the beam-steering solution - within a pre-defined set - maximizing the signal to interference ratio, yields the best performance. The use of such a solution however could be impractical due to the long time required by the exhaustive beam-searching phase, especially in the joint bidirectional-beamforming case.

If accurate localization of the mobile users is available, ray tracing can be used as a real-time tool to estimate the directional characteristics of the channel and restrict the search domain in order to speed-up the beam-searching phase. According to the results collected in the investigated scenario, such a solution is likely to offer promising results, with an average degradation in terms of SINR of about 3-4 dBs compared to a truly exhaustive search, but with a processing time of two orders of magnitude lower.

ACKNOWLEDGMENT

Authors would like to thank Prof. R. Thomä and all researchers of his group at TU Ilmenau in Germany for the use of Channel Sounder and their help with measurements post-processing.

REFERENCES

[1] S. Kutty, D. Sen, "Beamforming for Millimeter Wave Communications: An Inclusive Survey", IEEE Comm. Surveys and Tutorials, vol. 18, No. 2, 2016;

[2] S. Sun, T.S. Rappaport, R. W. Heath, A. Nix, S. Rangan, "MIMO for Millimeter-Wave Wireless Communications: Beamforming, Spatial Multiplexing, or Both?", IEEE Comm. Magazine, vol. 52, no. 12, December 2014;

[3] A.F. Molisch, V.V. Ratnam, S. Han, Z. Z. Li, S. Nguyen, L. Li, K. Haneda, "Hybrid Beamforming for Massive MIMO: A Survey", IEEE Comm. Magazine, vol. 55, no. 9, September 2017;

[4] A.W. Mbugua, W. Fan, Y. Ji, F. Pedersen, "Millimeter Wave Multi-User Performance Evaluation Based on Measured Channels With Virtual Antenna Array Sounder", IEEE Access, vol. 6, pp. 12318-12326, March 2018;

[5] V. Raghavan, S. Subramanian, J. Cezanne, A. Sampath, "Directional Beamforming for Millimeter-Wave MIMO Systems", IEEE Global Comm. Conference, San Diego (CA), December 6-10, 2015;

[6] A. Sibille, C. Oestges, A. Zanella, "MIMO From Theory to Implementation", Elsevier Inc., 2011;

[7] S. Rangan, T. Rappaport, E. Erkip, "Millimeter-Wave Cellular Wireless Networks: potentials and Challenges", Proc. of the IEEE, vol. 102, no. 3, March 2014;

[8] M. Gapeyenko, A. Samuylov, M. Gerasimenko, D. Moltchanov, S. Singh, E. Aryafar, S. Yeh, N. Himayat, S. Andreev, Y. Koucheryavy, "Analysis of human body-blockage in urban millimeter wave cellular communications", IEEE Int. Conf. on Communications, Kuala Lumpur (MY),May 22-27, 2016;

[9] G.R. MacCartney, S. Deng, S. Sun, T. S. Rappaport, "Millimeter-Wave Human Blockage at 73 GHz with a Simple Double Knife-Edge Diffraction Model and Extension for Directional Antennas", IEEE Veh. Tech. Conf., Montreal (CDN), September 18-21, 2016;

[10] A. Goldsmith, "Wireless Communications", Cambridge University Press, 2005;

[11] T. S. Rappaport, F. Gutierrez, E. Ben-Dor, J. N. Murdock, Y. Qiao, J. I. Tamir, "Broadband Millimeter-Wave Propagation Measurements and Models Using Adaptive-Beam Antennas for Outdoor Urban Cellular Communications" IEEE Trans. Antennas and Propagation, vol. 61, no. 4, pp. 1850-1859, April 2013;

[12] H. Weingarten, Y. Steinberg, S. Shamai, "The capacity region of the Gaussian MIMO broadcast channel", Proc. IEEE Int. Symp. Inf. Theory, Chicago (IL), June 27 – July 2, 2004;

[13] T. Yoo, A. Goldsmith, "Optimality of Zero-Forcing Beamforming with Multiuser Diversity", IEEE Int. Conf. on Communications, Seoul (KR), 16-20 May 2005;

[14] "802.11ac-2013 - IEEE Standard for Information technology - Telecommunications and information exchange between systems Local and metropolitan area networks - Specific requirements - Part 11: Wireless LAN Medium Access Control (MAC) and Physical Layer (PHY) Specifications - Amendment 4: Enhancements for Very High Throughput for Operation in Bands below 6 GHz", IEEE 2013;

[15] Q.H. Spencer, C.B. Peel, A.L. Swindlehurst, M. Haardt, "An Introduction to the Multi-User MIMO Link", IEEE Comm. Magazine, vol. 42, no. 10, pp. 60-67, October 2004;

[16] M. R. Akdeniz, Y.Liu; M. K. Samimi; S. Sun ; S. Rangan ; T. S. Rappaport, E. Erkip, "Millimeter Wave Channel Modeling and Cellular Capacity Evaluation," in IEEE Journal on Selected Areas in Communications, vol. 32, no. 6, pp. 1164-1179, June 2014;

[17] D. Gesbert, M. Kountouris, R.W. Heath Jr., C-B. Chae, T. Salzer, "Shifting the MIMO Paradigm", IEEE Sig. Proc. Magazine, vol. 24, No. 5, pp. 36-46, September 2007;

[18] E. Bjornson, B. Ottersten, "Optimal Multiuser Transmit Beamforming: A Difficult Problem with a Simple Solution Structure", IEEE Signal Proc. Magazine, vol. 31, no. 4, pp. 142-148, July 2014;

[19] T. Nitsche, C. Cordeiro, A. B. Flores, E.W: Knightly, E. Perahia, J.C. Widmer, "IEEE 802.11ad: directional 60 GHz communication for multi-Gigabit-per-second Wi-Fi", IEEE Comm. Magazine, vol. 52, no. 12, December 2014;

[20] S.T. Valduga, L. Deneire, A.L.F. de Almeida, T.F. Maciel, R. Aparicio-Pardo, "Low Complexity Beam Selection for Sparse Massive MIMO Systems", Int. Symposium on Wireless Comm. Systems, Bologna (IT), August 28-31, 2017;

[21] M. Shehata, M. Helard, M. Crussiere, A. Roze and C. Langlais, "Angular Based Beamforming and Power Allocation Framework in a Multi-User Millimeter-Wave Massive MIMO System", IEEE 87th Veh. Tech. Conference, Porto (PT), June 3-6, 2018;

[22] J-C. Chen, "Efficient Codebook-Based Beamforming Algorithmfor Millimeter-Wave Massive MIMO Systems", IEEE Trans. on Veh. Tech., vol. 66, no. 9, pp. 7809-7817, September 2017;

[23] S.Y. Seidel, T.S. Rappaport, "A ray tracing technique to predict path loss and delay spread inside buildings", Global Telecomm. Conf., Orlando (FL), December 6-9, 1992;

[24] J. W. Wallace, W. Ahmad, Y. Yang, R. Mehmood, M. A. Jensen, "A Comparison of Indoor MIMO Measurements and Ray-Tracing at 24 GHz and 2.55 GHz", IEEE Trans. Antennas Propagation, vol. 65 no. 12, pp. 6656-6668, Dec. 2017;

[25] Y. Corre, Y. Lostanlen, "3D urban propagation model for large ray-tracing computation", Int. Conf. on Electromagnetics in Advanced Applications, Torino (IT), September 17-21, 2007;

[26] F. Fuschini, H. El-Sallabi, V. Degli Esposti, L. Vuokko, D. Guiducci, P. Vainikainen, "Analysis of Multipath Propagation in Urban Environment Through Multidimensional Measurements and Advanced Ray Tracing Simulation", IEEE Trans. Antennas Propagation, vol. 56, no. 3, pp. 848-857, March 2008;

[27] T. Rautiainen, R. Hoppe, G. Wolfle, "Measurements and 3D Ray Tracing Propagation Predictions of Channel Characteristics in Indoor Environments", IEEE 18th Int. Symposium on Personal, Indoor, and Mobile Radio Comm., Athens (GR), 3-7 September 2007;

[28] F. Fuschini, S. Häfner, M. Zoli, R. Müller, E. M. Vitucci, D. Dupleich, M. Barbiroli, J. Luo, E. Schulz, V. Degli-Esposti, R.S. Thomä, "Analysis of In-Room mm-Wave Propagation: Directional Channel Measurements and Ray Tracing Simulations," J. Infrared Millim. Terahertz Waves, vol. 38, no. 6, pp. 727-744, June 2017;

[29] V. Degli-Esposti, F. Fuschini, E. M. Vitucci, M. Barbiroli, M. Zoli, L. Tian, X. Yin, D. Dupleich, R. Muller, C. Schneider, R.S. Thoma, "Ray-tracing based mm-wave beamforming assessment," IEEE Access, vol. 2, pp. 1314 – 1325, Nov. 2014;

[30] A. Karstensen, W. Fan, F. Zhang, J. Ø. Nielsen, and G. F. Pedersen, "Analysis of Simulated and Measured Indoor Channels for mm-Wave Beamforming Applications," Hindawi International Journal of Antennas and Propagation, Vol. 2018, 17 pages, January 2018;

[31] S. Häfner, D. A. Dupleich, R. Müller, C. Schneider and R. S. Thomä, "Ultra-Wideband Channel Sounder for Measurements at 70 GHz," in Proc. of IEEE 81st Veh.Tech.Conf., Glasgow (UK), pp. 1–5, 11–14 May 2015;

[32] V. Degli-Esposti, F. Fuschini, E. M. Vitucci, G. Falciasecca, "Measurement and modelling of scattering from buildings", IEEE Trans. Antennas Propagat., vol.55, no.1, pp.143–153, Jan. 2007;

[33] F. Gil, A. R. Claro, J. M. Ferreira, C. Pardelinha, L. M. Correia, "A 3D interpolation method for base-station-antenna radiation patterns," IEEE Antennas Propagat. Magazine, vol. 43, no.2, pp. 132-137, Feb. 2001;

[34] T. Petrita, A. Ignea, "A new method for interpolation of 3D antenna pattern from 2D plane patterns," in Proc. of 2012 10th International Symposium on Electronics and Telecommunications, pp. 393 – 396, Timisoara (RO), November 15-16, 2012;

[35] E. Aryafar, N. Anand, T. Salonidis, E.W. Knightly, "Design and Experimental Evaluation of Multi-User Beamforming in Wireless LANs", Proc. of the 16th Int. Conf. on Mobile Computing Networking, Chicago (IL), September 20-24, 2010;

[36] N. Li, Z. Wei, J. Geng, L. Sang, D. Yang, "Multiuser Hybrid Beamforming for Max-Min SINR Problem under 60 GHz Wireless Channel", IEEE 25th Int. Symposium on Personal, Indoor and Mobile Radio Comm. (PIMRC), Washington (DC), September 2-5, 2014;

[37] K. Witrisal, P. Meissner, E. Leitinger, Y. Shen, C. Gustafson, F. Tufvesson, K. Haneda, D. Dardari, A. Molisch, A. Conti, and M. Z. Win, "High-accuracy localization for assisted living: 5G systems will turn multipath channels from foe to friend," IEEE Signal Process. Mag., vol. 33, no. 2, pp. 59–70, Mar. 2016.

[38] M. Koivisto, A. Hakkarainen, M. Costa, P.Kela, K. Leppanen, M. Valkama, "High-Efficiency Device Positioning and Location Aware Communications in Dense 5G Networks", IEEE Comm. Magazine, vol. 55, no. 8, pp. 188-195, August 2017;

[39] R. Di Taranto, S. Muppirisetty, R. Raulefs, D.T.M. Slock, T. Svensson, H. Wymeersch, "Location-Aware Communications for 5G Networks", IEEE Signal Proc. Magazine, vol. 31, no. 6, pp. 102-112, November 2014;

[40] Z. Yun, S.Y. Lim, M. Iskander, "Propagation Prediction in Urban Areas Using Geospatial Data Available on the Internet", IEEE Ant. and Propagat. Society Int. Symposium, San Diego (CA), July 5-11, 2008;

[41] J. Jarvelainen, K. Haneda, M. Kyro, V-M. Kolmonen, J. Takada, H. Hagivara, "60 GHz radio wave propagation prediction in a hospital environment using an accurate room structural model", Loughborough Ant. & Propagat. Conference, Loughborough (UK), November 12-13, 2012;